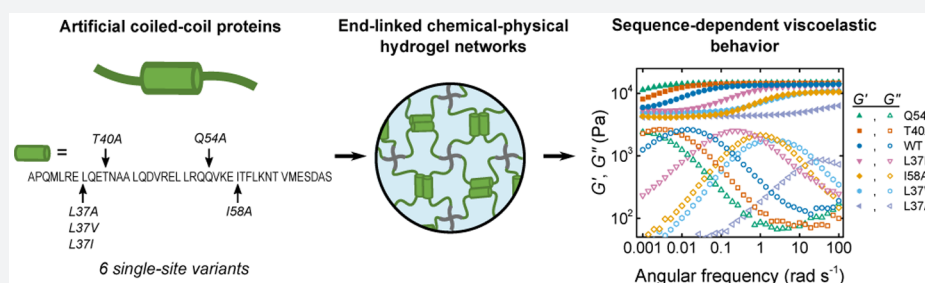


Engineering the Dynamic Properties of Protein Networks through Sequence Variation

Lawrence J. Dooling and David A. Tirrell*

Division of Chemistry and Chemical Engineering, California Institute of Technology, 1200 East California Boulevard, Pasadena, California 91125, United States

Supporting Information



ABSTRACT: The dynamic behavior of macromolecular networks dominates the mechanical properties of soft materials and influences biological processes at multiple length scales. In hydrogels prepared from self-assembling artificial proteins, stress relaxation and energy dissipation arise from the transient character of physical network junctions. Here we show that subtle changes in sequence can be used to program the relaxation behavior of end-linked networks of engineered coiled-coil proteins. Single-site substitutions in the coiled-coil domains caused shifts in relaxation time over 5 orders of magnitude as demonstrated by dynamic oscillatory shear rheometry and stress relaxation measurements. Networks with multiple relaxation time scales were also engineered. This work demonstrates how time-dependent mechanical responses of macromolecular materials can be encoded in genetic information.

INTRODUCTION

Cellular behaviors such as proliferation,¹ spreading and migration,² and differentiation³ are regulated in part by the stiffness of the local tissue microenvironment. These observations have prompted substantial efforts to design materials with tunable mechanical properties for applications in tissue engineering and for fundamental investigations of cellular mechanotransduction and cell-matrix interaction. The stiffness of biomaterials is typically characterized by an elastic modulus relating the deformation and stress at small strains. The moduli of materials used in cell culture can vary from less than 1 kPa for soft gels⁴ to more than 1 GPa for glass and tissue culture polystyrene.⁵ Several recent studies have suggested that in addition to the elasticity of a material, its viscous or dissipative properties may also influence cellular behavior.^{6–9} If we are to understand these phenomena and harness them for use in tissue engineering and regenerative medicine, we must develop reliable strategies for the design of materials with predictable and tunable dynamic properties.

Dynamic materials have been engineered both from synthetic polymers and from proteins. Examples of dynamic polymer networks include viscoelastic gels and elastomers cross-linked by hydrophobic interactions,¹⁰ hydrogen bonds,¹¹ metal–ligand complexes,^{12–15} and dynamic covalent bonds.^{16,17} Stress relaxation and energy dissipation in these materials arise from the transient nature of at least some of the network junctions,

and the characteristic relaxation time scales can therefore be tuned by modifying the lifetime of the transient cross-links. In protein networks, dynamic properties emerge from transient association of complementary domains on neighboring chains. Hydrogels cross-linked by coiled-coil domains^{18–21} are among the most thoroughly studied examples of dynamic protein networks. The lifetime of a coiled-coil cross-link is related to the characteristic time (τ_e) for exchange of individual strands between coiled-coil bundles. Although exchange times have been reported only for a small number of coiled coils derived from transcription factors, structural proteins, and designed peptides, these measurements reveal a wide range of exchange rates ($(\tau_e) \approx 1$ s to $>10^4$ s) relevant to engineering relaxation behavior in soft materials.^{19,22–25} Furthermore, coiled-coil exchange dynamics are sensitive to pH,¹⁹ allosteric regulation by binding partners,²⁴ and mutation of the amino acid sequence.²⁵ The effects of mutations are particularly intriguing as they suggest that the relaxation behavior of protein networks might be encoded in genetic information.

To test this idea, we prepared a set of seven artificial proteins that differ from one another by a single amino acid residue located in a helical domain designed to form coiled-coil bundles. Association of these domains in end-linked hydrogel

Received: July 21, 2016

Published: October 18, 2016

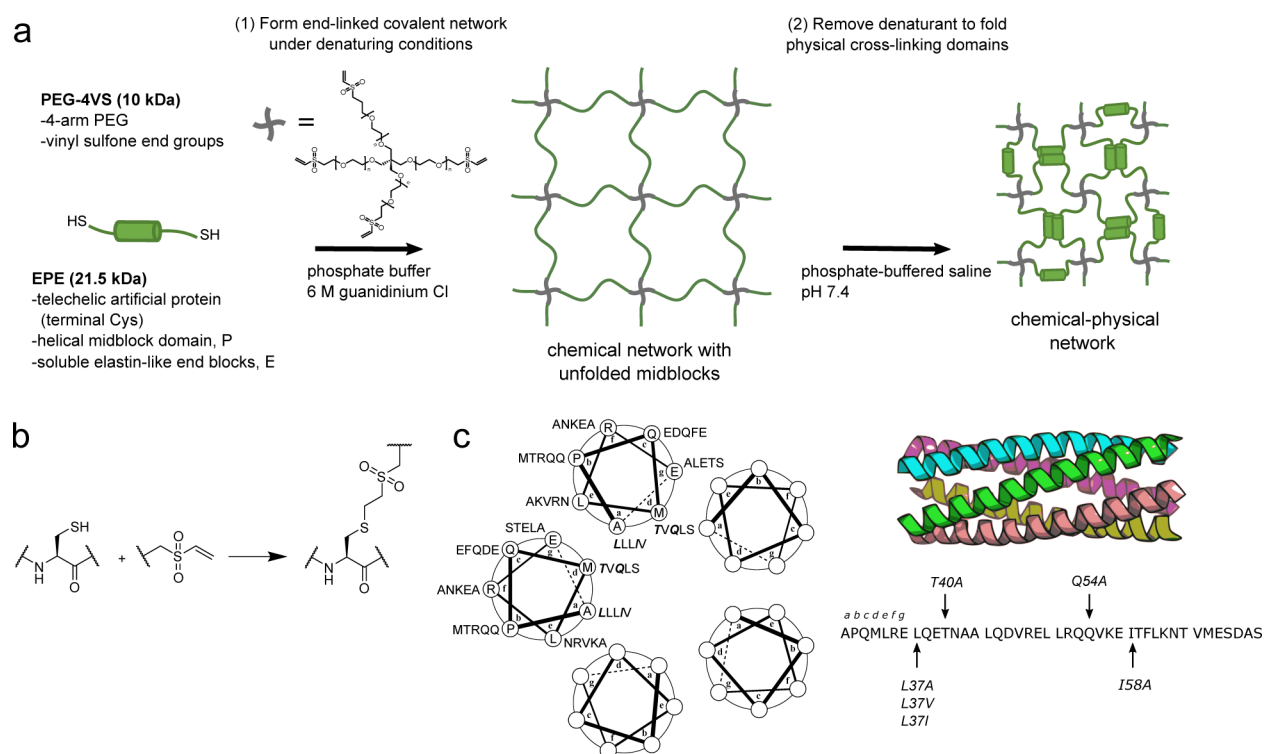


Figure 1. Cross-linking scheme and sequence of P domain. (a) Hydrogels are formed by end-linking artificial protein EPE with four-arm PEG vinyl sulfone. The reaction is carried out under denaturing conditions (6 M guanidinium chloride). Removal of the denaturant allows physical cross-links to form between EPE midblock domains. (b) End-linking is accomplished by formation of a thioether bond between cysteine residues located at the termini of EPE and the vinyl sulfone groups at the end of each arm of the four-arm PEG. (c) The midblock domain P in EPE forms homopentameric coiled coils (PDB 1VDF²⁸). Below the structure, the amino acid sequence of the P domain is divided into six heptad repeats using the conventional *abcdefg* notation for coiled-coil peptides. The mutated residues leucine 37, threonine 40, glutamine 54, and isoleucine 58 are noted with arrows and bolded in the helical wheel diagram. For clarity, midblock association in (a) is shown as dimeric association of the helical domains.

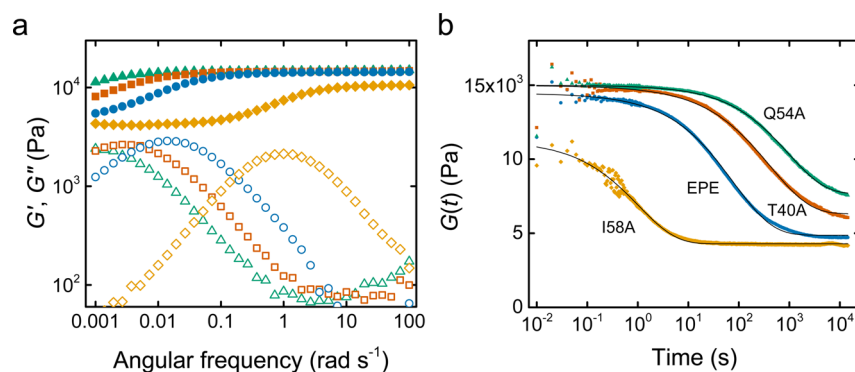


Figure 2. Rheology of EPE and variants Q54A, T40A, and I58A. (a) Dynamic oscillatory frequency sweeps showing storage moduli (G' , filled symbols) and loss moduli (G'' , open symbols) at 2% strain amplitude, 25 °C. In gels prepared from the Q54A (triangles) and T40A (squares) variants, the G' and G'' curves are shifted to lower frequencies relative to those for EPE gels (circles). In gels prepared from the I58A (diamonds) variant, the G' and G'' curves are shifted to higher frequencies relative to EPE gels. (b) The same trend is observed in stress relaxation experiments in which gels were subjected to a 2% step strain at 25 °C. The characteristic relaxation times determined from fits of the stretched exponential model (solid black lines) follow the trend $\tau_{\text{Q54A}} > \tau_{\text{T40A}} > \tau_{\text{EPE}} > \tau_{\text{I58A}}$.

networks resulted in transient physical cross-linking and viscoelastic behavior that was strikingly dependent on protein sequence. Networks prepared from mixtures of proteins exhibited more complex dynamic behavior characterized by multiple relaxation time scales.

RESULTS AND DISCUSSION

Recombinant artificial proteins form hydrogel networks by physical cross-linking through association of structured

domains on neighboring chains or by covalent cross-linking between amino acid side chain functional groups. We showed previously that the combination of covalent and physical cross-linking in networks prepared from a telechelic artificial protein denoted EPE gives rise to distinctive viscoelastic behavior.²⁶ EPE contains elastin-like end blocks (E), a helical midblock domain (P), and N- and C-terminal cysteine residues.²⁶ The P domain is derived from the N-terminal sequence of cartilage oligomeric matrix protein, which forms pentameric coiled coils that have been characterized thoroughly by biochemical

methods including X-ray crystallography, analytical ultracentrifugation, and circular dichroism spectroscopy^{27,28} and used previously to cross-link physical protein gels.^{29,30} Networks were formed by addition of the cysteine thiols in EPE to the terminal vinyl sulfone units of a four-arm poly(ethylene glycol) star polymer (PEG-4VS) (Figure 1a,b).³¹ Covalent end-linking was accomplished by mixing solutions of EPE and PEG-4VS under denaturing conditions (6 M guanidinium chloride) in which the helical midblock domains are expected to be unfolded. After swelling in phosphate-buffered saline to remove the denaturant, the midblock domains on neighboring chains associate to form physical cross-links (Figure 1a,c). Frequency-sweep small-amplitude oscillatory shear (SAOS) tests of EPE hydrogels at 2% strain amplitude (Figure 2a) reveal a storage modulus (G') that transitions between high- and low-frequency plateau values, with the midpoint of the transition coinciding with a maximum in the loss modulus (G''). When the network is deformed at high oscillation frequency, stress is stored in the short chain segments that connect the covalent cross-link points and the associating midblock domains. When the network is deformed at low frequency, the coiled-coil domains are no longer elastically effective, and stress is stored only in the longer chain segments that link covalent network junctions. This behavior is also evident in stress relaxation experiments in which the gel is subjected to a 2% step strain (Figure 2b). As the coiled-coil network junctions re-equilibrate in response to deformation of the gel, the relaxation function $G(t)$ decays to an equilibrium modulus associated with the covalent network.

To explore the relationship between protein sequence and the macroscopic properties of protein networks, we prepared six EPE variants that each contained a single point mutation in the P domain. The mutations were selected on the basis of the work of Gunasekar et al., in which alanine scanning mutagenesis was performed on the *a* and *d* positions that lie along the interhelical interfaces of the coiled-coil bundle.³² Replacement of aliphatic residues in P (at Leu 37, Leu 44, Val 47, Leu 51, or Ile 58) by alanine destabilized the helical structure, while mutations of polar residues (Thr 40 or Gln 54) to alanine resulted in stabilization. An increase in thermal stability was also observed when Gln 54 was mutated to leucine³³ or isoleucine.³⁴ We previously found that hydrogels prepared from an EPE variant containing the L44A mutation showed no evidence of physical cross-linking,²⁶ but the other mutations were not explored. Here, six EPE variants (designated T40A, Q54A, I58A, L37A, L37V, and L37I) (Figure 1c and Table S2) were expressed in *Escherichia coli* strain BL21 and purified by inverse temperature cycling (Figure S1). The proteins were reduced, desalted, and stored under inert atmosphere at $-80\text{ }^{\circ}\text{C}$ to ensure high free-thiol content, which was measured by Ellman's assay³⁵ to be between 83 and 91% for all EPE variants (Figure S2 and Table S4). The results of Ellman's assay were consistent with analysis by nonreducing SDS-PAGE, which confirmed that the proteins were monomeric (Figure S3 and Table S3). The molar masses of the proteins were verified by electrospray ionization mass spectrometry (ESI-MS) (Table S5).

We assessed the rheological behavior of hydrogels prepared by treating T40A, Q54A, or I58A with PEG-4VS. While these point mutations were each shown to affect the melting temperature and fractional helicity of the P coiled coil, they did not alter the pentameric oligomerization state,³² and therefore the mutated coiled coils were still expected to form physical cross-links when end-linked into covalent networks. In

SAOS frequency sweep experiments (Figure 2a), T40A and Q54A gels exhibit high-frequency plateaus in G' that are similar in magnitude to the high-frequency plateau values observed for EPE gels. In these variants, however, the plateau behavior extends to lower frequencies than in EPE gels. The maximum in G'' also occurs at a lower frequency (0.003 rad s^{-1}) in T40A gels. In Q54A gels, a maximum in G'' was not observed in the experimental frequency range, but the shape of the curve suggests a maximum between 10^{-4} and $10^{-3}\text{ rad s}^{-1}$. These observations are consistent with slower relaxation of coiled-coiled domains containing T40A or Q54A mutations. In hydrogels prepared from I58A, the opposite behavior is observed. Both the transition zone between the plateaus in G' and the maximum in G'' occur at higher frequencies than in EPE gels, meaning that relaxation of physical cross-links is faster in these materials. These experiments reveal a trend in the relaxation times of these materials ($Q54A > T40A > EPE > I58A$) that parallels the trend in thermal stability reported by Gunasekar et al.³²

To investigate the long time behavior of the more stable EPE variants T40A and Q54A, we performed stress relaxation experiments at 2% strain (Figure 2b). The relaxation function $G(t)$ was fit with the stretched exponential model previously used for physical protein hydrogels²⁰ and modified here to account for the permanent covalent network. The stress relaxation experiments confirmed the trend observed in the SAOS frequency sweeps and allowed us to determine the mean relaxation time for each material, which varied from approximately 1 s for I58A gels to more than 1500 s for Q54A gels (Table 1). In light of the fact that each of the three

Table 1. Plateau Moduli, $G(t = 0)$ and $G(t \rightarrow \infty)$, and Characteristic Relaxation Time, $\langle \tau \rangle$, for EPE and the Six Single-Site Mutant Variants Were Determined by Fitting the Data to a Stretched Exponential Model^a

protein	$\langle \tau \rangle$ (s)	$G(t = 0)$ (kPa)	$G(t \rightarrow \infty)$ (kPa)	$M_c(t \rightarrow \infty)$ (kg mol ⁻¹)
L37A	0.22 ± 0.13	6.9 ± 0.6	4.7 ± 1.0	28.1
L37V	1.02 ± 0.14	12.1 ± 0.4	5.1 ± 0.1	28.2
I58A	1.70 ± 0.15	11.1 ± 0.1	4.5 ± 0.3	32.0
L37I	9.83 ± 1.19	13.6 ± 0.4	5.2 ± 0.7	30.4
EPE	134 ± 8	14.0 ± 0.6	4.6 ± 0.2	32.3
T40A	762 ± 62	14.7 ± 0.2	5.7 ± 0.6	26.5
Q54A	1608 ± 135	14.8 ± 0.9	6.8 ± 0.8	23.0

^aL37A was not well fit by a stretched exponential model, so the single exponential model is reported instead ($n = 3$, avg s.d.). The equilibrium modulus $G(t \rightarrow \infty)$ was used to determine the average molecular weight between covalent cross-links (M_c). The expected value of M_c based on the protein molecular weight and the molecular weight of two arms of the PEG-4VS cross-linker is 26.5 kg mol^{-1} .

“mutant” materials differs from EPE by only a single amino acid residue, the results illustrate the remarkable sensitivity of the macroscopic stress relaxation time to the details of the molecular structure. The more stable variants Q54A and T40A are slightly stiffer than I58A and slightly less swollen (Figure S4). Both observations can be explained by a greater fraction of folded P domains in the more stable variants. The average molecular weight between covalent cross-links (M_c) was estimated using the phantom network approximation (Table 1); the value of M_c for each variant is close to the theoretical molecular weight between cross-links (26.5 kg mol^{-1}) based on the protein and cross-linker molar masses.

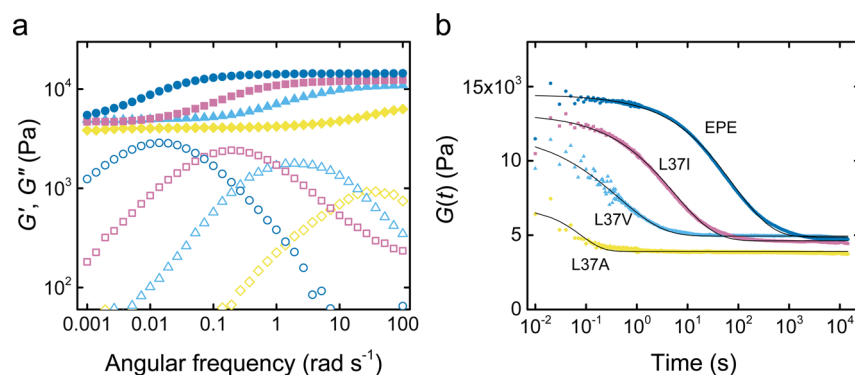


Figure 3. Rheology of EPE variants with point mutations at position 37 (L37I, L37V, and L37A). (a) Dynamic oscillatory frequency sweeps showing storage moduli (G' , filled symbols) and loss moduli (G'' , open symbols) at 2% strain amplitude, 25 °C. In gels prepared from the L37I (squares), L37V (triangles), and L37A (diamonds) variants, the G' and G'' curves are shifted to higher frequencies relative to those for EPE gels (circles). Similar behavior was observed when L37V was subjected to rheological analysis at temperatures of 5, 15, and 35 °C (Figure S5). (b) The same trend in the relaxation time is observed in stress relaxation experiments in which gels were subjected to a 2% step strain at 25 °C. The characteristic relaxation times were determined from fits of the stretched exponential model for EPE, L37I, and L37V (solid black lines). The relaxation function for L37A was not well fit by the stretched exponential model, so the single exponential fit is shown instead. The trend in the characteristic relaxation time is $\tau_{\text{EPE}} > \tau_{\text{L37I}} > \tau_{\text{L37V}} > \tau_{\text{L37A}}$.

We further investigated how sequence variation in the coiled-coil domain could be used to program the relaxation behavior of protein gels by designing EPE variants containing point mutations at leucine 37. Mutation of this residue to alanine by Gunasekar et al. decreased the helicity of the P domain from 70% in the wild-type peptide to 22% in the mutant.³² In hydrogels prepared by cross-linking L37A with PEG-4VS, G' is independent of the oscillation frequency below approximately 5 rad s^{-1} but increases with increasing frequency above this value (Figure 3a). The increase in G' is accompanied by a local maximum in G'' . As in gels prepared from I58A, the shifts of the G' and G'' curves to higher frequencies relative to EPE suggest that transient physical cross-links are still present in L37A gels, but exchange more rapidly than in EPE. The relaxation time of the L37A network, which is estimated as 0.22 s from the stress relaxation experiment (Figure 3b and Table 1), is approximately 3 orders of magnitude smaller than the relaxation time of EPE gels. This effect mirrors the shift in the strand exchange time that accompanies single leucine-to-alanine substitutions in leucine-zipper peptides (~ 1800 s to ~ 1 s).²⁵

The accessible surface area of the alanine side chain is approximately one-half that of leucine (67 Å² versus 137 Å²),³⁶ and the loss of hydrophobic contacts at position 37 of the P domain likely destabilizes the coiled-coil aggregates and enables faster network relaxation. This hypothesis led us to prepare EPE variants containing L37V and L37I mutations. The accessible surface area of valine (117 Å²) lies between those of leucine and alanine.³⁶ Isoleucine has an accessible surface area (140 Å²) similar to that of leucine, but its side chain is branched at the β - rather than the γ -carbon.³⁶ In both L37V and L37I gels, the curves for G' and G'' are shifted to higher frequencies relative to EPE gels, but the shift is not as large as that observed for L37A (Figure 3a). The characteristic relaxation times for L37V and L37I networks are on the order of 1 and 10 s, respectively (Figure 3b and Table 1). Thus, the relaxation times for EPE and its variants modified at position 37 decrease in the order EPE > L37I > L37V > L37A and illustrate how rational design of the coiled-coil cross-linking domains can be used to program the relaxation behavior of artificial protein networks.

When gels prepared from EPE and its variants are swollen in buffer containing 6 M guanidinium chloride (a protein denaturant), the coiled-coil domains are disrupted, but the gels remain cross-linked through covalent bonds. The storage moduli of gels swollen in denaturing buffers are nearly independent of the oscillation frequency (Figure S6a), as expected for highly swollen, covalent elastic networks. Addition of guanidinium chloride also increases the extent of swelling (Figure S6b), consistent with a loss of physical cross-linking. Because association between P domains is disrupted by the denaturant, the effects of sequence variation are lost and the protein variants are no longer distinguishable (Figure S6a).

The approach developed here can also be used to design materials with more complex relaxation dynamics. We imagined that it should be possible to observe multiple, distinct relaxation processes in gels made by cross-linking mixtures of proteins that meet two criteria: The proteins must have orthogonal physical cross-linking domains, and the relaxation times for these domains must be well separated. To construct such a network, we designed an artificial protein (designated EAE) that contains an artificial coiled-coil domain (A) in place of P (Figure 4a). Shen et al. developed physical hydrogels from telechelic artificial proteins with terminal A and P domains and demonstrated that these domains do not associate with one another.³⁰ Hydrogels prepared by cross-linking EAE with PEG-4VS exhibit relaxation behavior (Figure 4c,d) similar to that of Q54A. This suggests that physical cross-links formed by the A domain are longer-lived than those formed by P. To engineer gels that exhibit distinct relaxation times, we paired EAE and L37V in a covalent network cross-linked with PEG-4VS (Figure 4b, (iv)). The single L37V mutation in P is not expected to affect its orthogonality with A, and the relaxation times of the individual EAE and L37V networks are separated by approximately 3 orders of magnitude.

Hydrogels were prepared by cross-linking equimolar mixtures of EAE and L37V under denaturing conditions and then swollen to equilibrium in phosphate-buffered saline, pH 7.4. In both SAOS frequency sweep experiments and stress relaxation experiments (Figure 4c,d and Figure S7a), distinct relaxation processes are observed on time scales that correspond to those of the individual L37V and A domains.

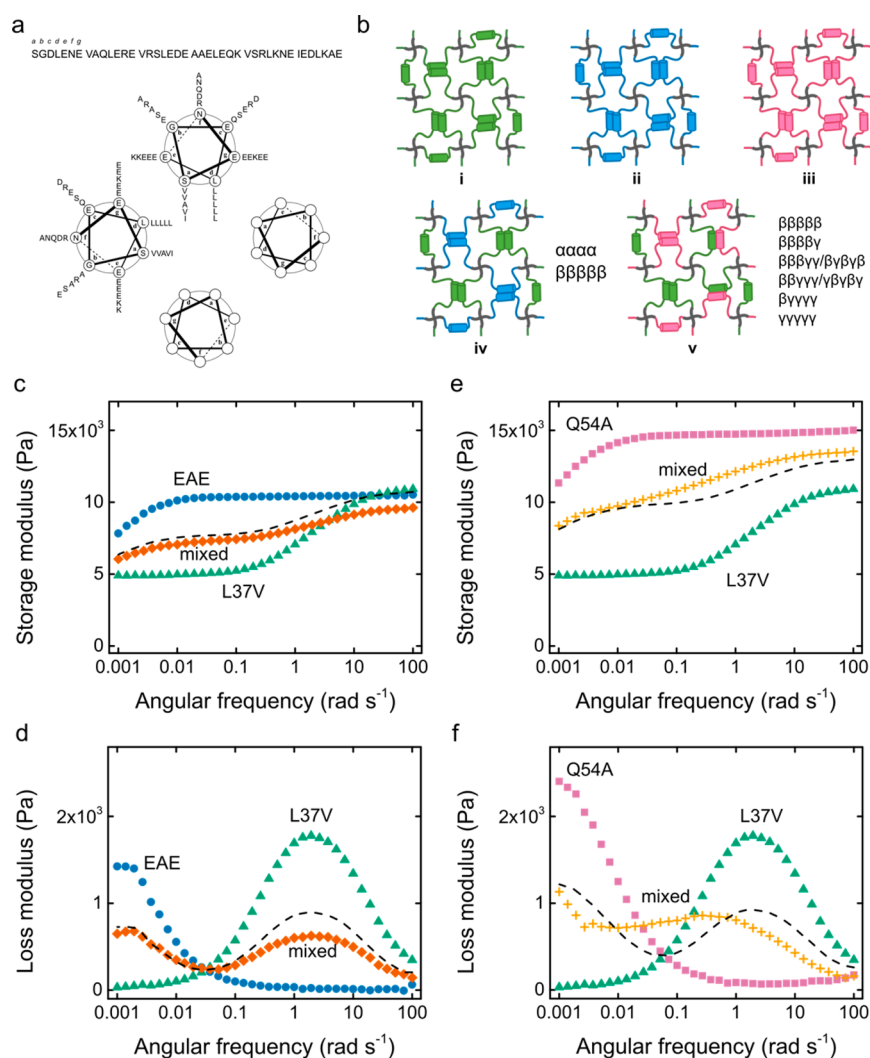


Figure 4. Chemical-physical protein networks with multiple relaxation times. (a) Sequence of the A coiled-coil domain and helical wheel representation of a parallel A homotetramer (antiparallel orientations are also possible). (b) Schematic representation of chemical-physical protein networks prepared from a single artificial protein (i. L37V, ii. EAE, iii. Q54A) or two artificial proteins with different associative midblocks (iv. L37V:EAE, v. L37V:Q54A). In network iv, the coiled coils are orthogonal to one another, and two types of physical cross-links are present, i.e., tetramers of α and pentamers of β . In network v, mixed species cross-linking is possible, i.e., through formation of eight different pentamers of β and γ . (c) Storage moduli and (d) loss moduli of EAE gels (circles), L37V gels (triangles), and gels prepared by cross-linking an equimolar mixture of EAE and L37V (diamonds). (e) Storage moduli and (f) loss moduli of Q54A gels (squares), L37V gels (triangles), and gels prepared by cross-linking an equimolar mixture of Q54A and L37V (crosses). The dashed lines in (c–f) represent the theoretical averages of G' and G'' calculated from the curves for the single protein networks shown in those panels.

These processes are separated by plateau values in G' and $G''(t)$ at intermediate values of the frequency and time, respectively. The high-frequency plateau reflects the contributions of both L37V and A domains to the storage modulus, while the reduced plateau value of G' at intermediate frequencies reflects only the contributions of the longer-lived A domains. Finally, the low-frequency plateau arises from stress stored between the chemical cross-links on time scales greater than the dissociation times of both coiled-coil domains. The frequencies of the transitions between these plateaus coincide with local maxima in G'' . Notably, a local minimum in G'' in the L37V:EAE gel occurs near the intersection of the G'' curves of the individual L37V and EAE gels, consistent with the theoretical average of the two curves (Figure 4d and Figure S8).

A similar approach was used to prepare networks from mixtures of proteins that were not expected to exhibit orthogonal physical cross-linking (Figure 4b, (v)). While the

relaxation times in single protein networks prepared from L37V and Q54A are separated by several orders of magnitude, we expected mixed-species helical bundles to form in networks prepared from equimolar mixtures of the two proteins. In networks of this kind, eight combinations of strands are possible in pentameric aggregates of the modified P domains. Frequency sweep and stress relaxation experiments on L37V:Q54A gels reveal a broad distribution of relaxation times, in contrast to the two discrete relaxation processes observed in EAE:L37V gels (Figure 4e,f and Figure S7b). This difference is most evident by comparing the loss modulus of the L37V:Q54A network and the theoretical average value of G'' calculated from the G'' curves for the L37V and Q54A single protein networks; the clear local maxima and minimum expected from averaging the two curves are absent in L37V:Q54A gels (Figure 4d and Figure S8). A decrease in G' and an increase in G'' are observed at the lowest frequencies in

L37V:Q54A gels on the time scale characteristic of Q54A physical cross-links. This suggests that a significant number of homotypic Q54A cross-links form in this gel, which is perhaps not surprising given that Q54A is expected to have a higher fraction of folded midblock domains than L37V.³²

CONCLUSIONS

The sequence-structure-function paradigm has long guided our understanding of protein behavior and our efforts to design new proteins. Here we've shown how sequence variation can be used to engineer the dynamic mechanical behavior of protein networks. Dynamic materials are expected to play important roles in regulating cell and tissue behavior,^{6–9,37–39} and to exhibit enhanced toughness through programmed dissipation of the energy associated with mechanical deformation.⁴⁰ The use of molecular genetics to program relaxation behavior in soft materials will create important new opportunities in materials science, cell and tissue engineering, and regenerative medicine.

MATERIALS AND METHODS

Protein Expression and Purification. Construction of the pQE-80L plasmids encoding the EPE variants and EAE is described in the [Supporting Information](#). The artificial proteins were expressed in BL21 *Escherichia coli* (New England BioLabs, Ipswich, MA) and purified by methods similar to those previously published²⁵ with some modifications. Briefly, 1 L cultures were grown at 37 °C in Terrific broth containing 100 $\mu\text{g mL}^{-1}$ ampicillin (BioPioneer, San Diego, CA) to an optical density at 600 nm (OD_{600}) of 1. Isopropyl β -D-1-thiogalactopyranoside (IPTG) (BioPioneer) was added to a final concentration of 1 mM, and the cells were harvested 4 h later by centrifugation at 6000g for 8 min at 4 °C. The cells were frozen at a concentration of 0.5 g mL^{-1} in TEN buffer (10 mM Tris, 1 mM EDTA, 100 mM NaCl, pH 8.0) supplemented with 5% (v/v) glycerol, 0.1% (w/v) sodium deoxycholate (Sigma, St. Louis, MO), and 0.1% (v/v) TritonX-100 (Sigma). After being thawed, the lysate was treated with 10 $\mu\text{g mL}^{-1}$ DNaseI (Sigma), 5 $\mu\text{g mL}^{-1}$ RNaseA (Sigma), 5 mM MgCl_2 , and 1 mM phenylmethylsulfonyl fluoride (Gold Biotechnology, Olivette, MO) while shaking at 37 °C, 250 rpm for 30 min. The lysate was then sonicated for 5 min (2 s on, 2 s off, 30% power amplitude) (QSonica, Newton, CT) and allowed to rest for 2 h on ice. β -Mercaptoethanol (β ME) (Sigma) was added to the lysate at a final concentration of 1% (v/v) following sonication.

The target proteins were purified from the *E. coli* lysate by three rounds of temperature cycling.⁴¹ The lysate was centrifuged at 39000g for 1 h at 4 °C to remove insoluble proteins and cellular debris. Crystalline NaCl was added to the supernatant at a final concentration of 2 M followed by shaking at 250 rpm, 37 °C for 1 h. The aggregated proteins were collected by centrifugation at 39000g for 1 h at 37 °C and solubilized overnight at a concentration of 100 mg mL^{-1} in cold TEN buffer containing 1% (v/v) β ME. Two more cycles were completed with 30 min centrifugation spins. The β ME was omitted in the final resuspension step. Instead, 5 mM tris(hydroxypropyl)phosphine (THP) (Santa Cruz Biotechnology, Dallas, TX) was added, and the protein solution was incubated at 4 °C for 2 h. The purified protein was desalted into LC-MS grade water (Fluka, St. Louis, MO) using Zeba 7K MWCO columns (Thermo Fisher Scientific, Waltham, MA) and lyophilized for 4 days. The lyophilized protein was stored under argon at –80 °C or used immediately. Typical yields

were greater than 100 mg per liter of culture. Characterization of the artificial proteins by SDS-PAGE, mass spectrometry, and Ellman's assay is described in the [Supporting Information](#).

Hydrogel Cross-Linking and Swelling. The lyophilized artificial proteins were dissolved at a concentration of 150 mg mL^{-1} in degassed cross-linking buffer (0.1 M sodium phosphate, 6 M guanidinium chloride, 0.4 M triethanolamine, pH 7.4) by sonicating for 2 min in an ultrasonic bath. Bubbles were removed by centrifugation at 10000g for 1 min. The PEG-4VS cross-linker (Jenkem USA, Plano, TX) was dissolved at a concentration of 150 mg mL^{-1} in degassed 0.4 M triethanolamine, pH 7.4. Cross-linking was initiated by mixing the two solutions in a volumetric ratio that gave a 1:1 stoichiometry between the thiol and vinyl sulfone functional groups. The solution was vortexed to ensure homogeneous mixing and quickly pipetted onto a glass slide that was treated with SigmaCote (Sigma). A second treated glass slide was placed on top of the droplet and supported by spacers cut from a 1 mm thick rubber sheet (McMaster-Carr, Santa Fe Springs, CA). The slides were clamped together, and the gels were allowed to cure in the dark overnight.

Hydrogels prepared for rheological measurements were transferred to a dish containing 6 mL of phosphate-buffered saline (PBS) (1.5 mM KH_2PO_4 , 4.3 mM Na_2HPO_4 , 137 mM NaCl, 2.7 mM KCl, pH 7.4) plus 6 M guanidinium chloride. The gels were swollen in this buffer for 3 h before switching to PBS plus 3 M guanidinium chloride for 3 h, then PBS plus 2 M guanidinium chloride for 3 h, PBS plus 1 M guanidinium chloride for 3 h, and finally PBS. The gradual decrease in the guanidinium chloride concentration is intended to allow unreacted protein chains to diffuse out of the gel and to promote proper folding of the coiled-coil domains. For extended swelling in PBS (longer than 1 day), 0.02% (w/v) sodium azide (Sigma) was added to the buffer to inhibit microbial contamination. Measurement of the hydrogel mass swelling ratio is described in the [Supporting Information](#).

Rheology. Swollen hydrogels prepared from EPE, EAE, and EPE variants were characterized by small amplitude oscillatory shear rheology and shear stress relaxation on an ARES-RFS strain-controlled rheometer (TA Instruments, New Castle, DE). Gels were cut into disks with an 8 mm biopsy punch (Miltex, York, PA), loaded between the 8 mm parallel plate test geometry as previously described^{26,42} and equilibrated for 1 h. Frequency sweeps were acquired at 2% strain amplitude, 25 °C. Following the frequency sweep, a stress relaxation experiment was performed with a 2% step strain at 25 °C. For each stress relaxation experiment, the relaxation function $G(t)$ was fit with the stretched exponential previously used for physical protein hydrogels²⁰ and modified here with the parameter G_e to account for the contribution of the permanent covalent network.

$$G(t) = G \exp\left(-\left(\frac{t}{\tau_{\text{KWW}}}\right)^\beta\right) + G_e \quad (1)$$

The physical cross-linking is described by the parameter G as well as the relaxation time scale τ_{KWW} and the exponent β , which varies between 0 and 1. The mean relaxation time for each material is calculated from

$$\langle\tau\rangle = \frac{\tau_{\text{KWW}}}{\beta} \Gamma\left(\frac{1}{\beta}\right) \quad (2)$$

where $\Gamma\left(\frac{1}{\beta}\right)$ is the gamma function evaluated at β^{-1} .

For mixed protein networks, $G(t)$ was fit to a double stretched exponential model:

$$G(t) = G_1 \exp\left(-\left(\frac{t}{\tau_1}\right)^{\beta_1}\right) + G_2 \exp\left(-\left(\frac{t}{\tau_2}\right)^{\beta_2}\right) + G_e \quad (3)$$

which contains two exponential terms identical to those in eq 1 and an equilibrium modulus G_e representing the covalent cross-linking. To fit the experimental $G(t)$ data for the L37V:EAE and L37V:Q54A networks, the characteristic relaxation time scales (τ_1 and τ_2) and the stretching exponents (β_1 and β_2) were fixed at the values determined from the L37V and EAE or Q54A single protein networks, leaving G_1 , G_2 , and G_e as adjustable parameters.

The average molecular weight between covalent cross-links (M_c) was estimated by the phantom network approximation. For an ideal network cross-linked in the presence of solvent and swollen to equilibrium,

$$M_c = \left(1 - \frac{2}{f}\right) RT \frac{C_0}{G} \left(\frac{\varphi}{\varphi_0}\right)^{1/3} \quad (4)$$

where R is the universal gas constant, T is temperature in K, C_0 is the initial polymer concentration, G is the shear modulus, and φ and φ_0 are the equilibrium and initial polymer volume fractions.^{31,43,44} The PEG-4VS cross-linker has a functionality, f , of 4.⁴⁵ For each gel, the equilibrium polymer volume fraction was estimated from the mass swelling ratio and the initial polymer volume fraction was calculated from the total polymer concentration during cross-linking (150 mg mL⁻¹). For determining the average molecular weight of chain segments connected by covalent cross-links, the relevant value of the shear modulus was determined by evaluating the relaxation function $G(t)$ at $t \rightarrow \infty$. The theoretical molecular weight between covalent cross-links in the end-linked network was calculated by adding the molar mass of the protein (21.5 kg mol⁻¹) and the molar mass of two arms of the PEG-4VS polymer (2 × 5 kg mol⁻¹), for a total of 26.5 kg mol⁻¹.

■ ASSOCIATED CONTENT

Supporting Information

The Supporting Information is available free of charge on the ACS Publications website at DOI: 10.1021/acscentsci.6b00205.

Additional experimental details of cloning, protein characterization, and hydrogel swelling. Supporting Figures S1–S9. Supporting Tables S1–S5 (PDF)

■ AUTHOR INFORMATION

Corresponding Author

*E-mail: tirrell@caltech.edu.

Notes

The authors declare no competing financial interest.

■ ACKNOWLEDGMENTS

This work was supported by Grant Number DMR-1506483 from the Biomaterials Program of the U.S. National Science Foundation. We thank Professor Julia Kornfield for extensive access to the ARES-RFS rheometer and Dr. Mona Shahgholi of the Mass Spectrometry Facility of the Division of Chemistry

and Chemical Engineering at Caltech for assistance in measuring protein molar masses.

■ REFERENCES

- (1) Wang, H.-B.; Dembo, M.; Wang, Y.-L. Substrate flexibility regulates growth and apoptosis of normal but not transformed cells. *Am. J. Physiol. Cell Physiol.* **2000**, 279, C1345–C1350.
- (2) Pelham, R. J.; Wang, Y.-L. Cell locomotion and focal adhesions are regulated by substrate flexibility. *Proc. Natl. Acad. Sci. U. S. A.* **1997**, 94, 13661–13665.
- (3) Engler, A. J.; Sen, S.; Sweeney, H. L.; Discher, D. E. Matrix elasticity directs stem cell lineage specification. *Cell* **2006**, 126, 677–689.
- (4) Soofi, S. S.; Last, J. A.; Liliensiek, S. J.; Nealey, P. F.; Murphy, C. J. The elastic modulus of Matrigel as determined by atomic force microscopy. *J. Struct. Biol.* **2009**, 167, 216–219.
- (5) Ashby, M. F. *Materials Selection in Mechanical Design*, 3rd ed.; Elsevier Butterworth-Heinemann: Amsterdam, 2005.
- (6) Cameron, A. R.; Frith, J. E.; Cooper-White, J. J. The influence of substrate creep on mesenchymal stem cell behaviour and phenotype. *Biomaterials* **2011**, 32, 5979–5993.
- (7) Murrell, M.; Kamm, R.; Matsudaira, P. Substrate viscosity enhances correlation in epithelial sheet movement. *Biophys. J.* **2011**, 101, 297–306.
- (8) Chaudhuri, O.; Gu, L.; Darnell, M.; Klumpers, D.; Bencherif, S. A.; Weaver, J. C.; Huebsch, N.; Mooney, D. J., Substrate stress relaxation regulates cell spreading. *Nat. Commun.* **2015**, 6, 6365 DOI: 10.1038/ncomms7365.
- (9) Chaudhuri, O.; Gu, L.; Klumpers, D.; Darnell, M.; Bencherif, S. A.; Weaver, J. C.; Huebsch, N.; Lee, H.; Lippens, E.; Duda, G. N.; Mooney, D. J. Hydrogels with tunable stress relaxation regulate stem cell fate and activity. *Nat. Mater.* **2016**, 15, 326–334.
- (10) Annable, T.; Buscall, R.; Ettelaie, R.; Whittlestone, D. The rheology of solutions of associating polymers: Comparison of experimental behavior with transient network theory. *J. Rheol.* **1993**, 37, 695–726.
- (11) Sijbesma, R. P.; Beijer, F. H.; Brunsveld, L.; Folmer, B. J. B.; Hirschberg, J. H. K. K.; Lange, R. F. M.; Lowe, J. K. L.; Meijer, E. W. Reversible polymers formed from self-complementary monomers using quadruple hydrogen bonding. *Science* **1997**, 278, 1601–1604.
- (12) Fullenkamp, D. E.; He, L.; Barrett, D. G.; Burghardt, W. R.; Messersmith, P. B. Mussel-inspired histidine-based transient network metal coordination hydrogels. *Macromolecules* **2013**, 46, 1167–1174.
- (13) Menyo, M. S.; Hawker, C. J.; Waite, J. H. Rate-dependent stiffness and recovery in interpenetrating network hydrogels through sacrificial metal coordination bonds. *ACS Macro Lett.* **2015**, 4, 1200–1204.
- (14) Grindy, S. C.; Learsch, R.; Mozhdzhi, D.; Cheng, J.; Barrett, D. G.; Guan, Z.; Messersmith, P. B.; Holten-Andersen, N. Control of hierarchical polymer mechanics with bioinspired metal-coordination dynamics. *Nat. Mater.* **2015**, 14, 1210–1216.
- (15) Loveless, D. M.; Jeon, S. L.; Craig, S. L. Rational control of viscoelastic properties in multicomponent associative polymer networks. *Macromolecules* **2005**, 38, 10171–10177.
- (16) McKinnon, D. D.; Domaille, D. W.; Cha, J. N.; Anseth, K. S. Biophysically defined and cytocompatible covalently adaptable networks as viscoelastic 3D cell culture systems. *Adv. Mater.* **2014**, 26, 865–872.
- (17) Ying, H.; Zhang, Y.; Cheng, J. Dynamic urea bond for the design of reversible and self-healing polymers. *Nat. Commun.* **2014**, 5, DOI: 10.1038/ncomms4218.
- (18) Petka, W. A.; Harden, J. L.; McGrath, K. P.; Wirtz, D.; Tirrell, D. A. Reversible hydrogels from self-assembling artificial proteins. *Science* **1998**, 281, 389–392.
- (19) Shen, W.; Kornfield, J. A.; Tirrell, D. A. Dynamic properties of artificial protein hydrogels assembled through aggregation of leucine zipper peptide domains. *Macromolecules* **2007**, 40, 689–692.

- (20) Tang, S.; Wang, M.; Olsen, B. D. Anomalous self-diffusion and sticky Rouse dynamics in associative protein hydrogels. *J. Am. Chem. Soc.* **2015**, *137*, 3946–3957.
- (21) Xu, C.; Breedveld, V.; Kopeček, J. Reversible hydrogels from self-assembling genetically engineered protein block copolymers. *Biomacromolecules* **2005**, *6*, 1739–1749.
- (22) Ozeki, S.; Kato, T.; Holtzer, M. E.; Holtzer, A. The kinetics of chain exchange in two-chain coiled coils: $\alpha\alpha$ - and $\beta\beta$ -tropomyosin. *Biopolymers* **1991**, *31*, 957–966.
- (23) Park, S.-Y.; Quezada, C. M.; Bilwes, A. M.; Crane, B. R. Subunit exchange by CheA histidine kinases from the mesophile *Escherichia coli* and the thermophile *Thermotoga maritima*. *Biochemistry* **2004**, *43*, 2228–2240.
- (24) Patel, L. R.; Curran, T.; Kerppola, T. K. Energy transfer analysis of Fos-Jun dimerization and DNA binding. *Proc. Natl. Acad. Sci. U. S. A.* **1994**, *91*, 7360–7364.
- (25) Wendt, H.; Berger, C.; Baici, A.; Thomas, R. M.; Bosshard, H. R. Kinetics of folding of leucine zipper domains. *Biochemistry* **1995**, *34*, 4097–4107.
- (26) Dooling, L. J.; Buck, M. E.; Zhang, W.-B.; Tirrell, D. A. Programming molecular association and viscoelastic behavior in protein networks. *Adv. Mater.* **2016**, *28*, 4651–4657.
- (27) Efimov, V. P.; Lustig, A.; Engel, J. The thrombospondin-like chains of cartilage oligomeric matrix protein are assembled by a five-stranded α -helical bundle between residues 20 and 83. *FEBS Lett.* **1994**, *341*, 54–58.
- (28) Malashkevich, V. N.; Kammerer, R. A.; Efimov, V. P.; Schulthess, T.; Engel, J. The crystal structure of a five-stranded coiled coil in COMP: A prototype ion channel? *Science* **1996**, *274*, 761–765.
- (29) Olsen, B. D.; Kornfield, J. A.; Tirrell, D. A. Yielding behavior in injectable hydrogels from telechelic proteins. *Macromolecules* **2010**, *43*, 9094–9099.
- (30) Shen, W.; Zhang, K.; Kornfield, J. A.; Tirrell, D. A. Tuning the erosion rate of artificial protein hydrogels through control of network topology. *Nat. Mater.* **2006**, *5*, 153–158.
- (31) Lutolf, M. P.; Hubbell, J. A. Synthesis and physicochemical characterization of end-linked poly(ethylene glycol)-co-peptide hydrogels formed by Michael-type addition. *Biomacromolecules* **2003**, *4*, 713–722.
- (32) Gunasekar, S. K.; Asnani, M.; Limbad, C.; Haghpanah, J. S.; Hom, W.; Barra, H.; Nanda, S.; Lu, M.; Montclare, J. K. N-Terminal aliphatic residues dictate the structure, stability, assembly, and small molecule binding of the coiled-coil region of cartilage oligomeric matrix protein. *Biochemistry* **2009**, *48*, 8559–8567.
- (33) Terskikh, A. V.; Potekhin, S. A.; Melnik, T. N.; Kajava, A. V. Mutation Gln54Leu of the conserved polar residue in the interfacial coiled coil position (d) results in significant stabilization of the original structure of the COMP pentamerization domain. *Lett. Pept. Sci.* **1997**, *4*, 297–304.
- (34) Guo, Y.; Kammerer, R. A.; Engel, J. The unusually stable coiled-coil domain of COMP exhibits cold and heat denaturation in 4–6 M guanidinium chloride. *Biophys. Chem.* **2000**, *85*, 179–186.
- (35) Ellman, G. L. Tissue sulfhydryl groups. *Arch. Biochem. Biophys.* **1959**, *82*, 70–77.
- (36) Miller, S.; Janin, J.; Lesk, A. M.; Chothia, C. Interior and surface of monomeric proteins. *J. Mol. Biol.* **1987**, *196*, 641–656.
- (37) Liu, Y.; Liu, B.; Riesberg, J. J.; Shen, W. In situ forming physical hydrogels for three-dimensional tissue morphogenesis. *Macromol. Biosci.* **2011**, *11*, 1325–1330.
- (38) McKinnon, D. D.; Domaille, D. W.; Brown, T. E.; Kyburz, K. A.; Kiyotake, E.; Cha, J. N.; Anseth, K. S. Measuring cellular forces using bis-aliphatic hydrazone crosslinked stress-relaxing hydrogels. *Soft Matter* **2014**, *10*, 9230–9236.
- (39) Wang, H.; Heilshorn, S. C. Adaptable hydrogel networks with reversible linkages for tissue engineering. *Adv. Mater.* **2015**, *27*, 3717–3736.
- (40) Zhao, X. Multi-scale multi-mechanism design of tough hydrogels: building dissipation into stretchy networks. *Soft Matter* **2014**, *10*, 672–687.
- (41) McPherson, D. T.; Xu, J.; Urry, D. W. Product purification by reversible phase transition following *Escherichia coli* expression of genes encoding up to 251 repeats of the elastomeric pentapeptide GVGVP. *Protein Expression Purif.* **1996**, *7*, 51–57.
- (42) Meyvis, T. K. L.; De Smedt, S. C.; Demeester, J.; Hennink, W. E. Rheological monitoring of long-term degrading polymer hydrogels. *J. Rheol.* **1999**, *43*, 933–950.
- (43) Peppas, N. A.; Merrill, E. W. Crosslinked poly(vinyl alcohol) hydrogels as swollen elastic networks. *J. Appl. Polym. Sci.* **1977**, *21*, 1763–1770.
- (44) Gnanou, Y.; Hild, G.; Rempp, P. Molecular structure and elastic behavior of poly(ethylene oxide) networks swollen to equilibrium. *Macromolecules* **1987**, *20*, 1662–1671.
- (45) Rubinstein, M.; Colby, R. H. *Polymer Physics*; Oxford University Press: New York, 2003.